Chimie Douce Synthesis of a Layered Ammonium Zinc Molybdate

Doron Levin,† Stuart L. Soled,‡ and Jackie Y. Ying*,†

Department of Chemical Engineering, Massachusetts Institute of Technology, Cambridge, Massachusetts 02139, and Exxon Research and Engineering Company, Annandale, New Jersey 08801

Received September 12, 1995. Revised Manuscript Received January 17, 1996⊗

A layered ammonium zinc molybdate material was derived by a novel room-temperature *chimie douce* synthesis technique from a metastable mixed oxide prepared by calcination of a layered double hydroxide (LDH). The compound obtained, $(NH_4)HZn_2(OH)_2(MoO_4)_2$, is highly crystalline and retains the rhombohedral symmetry of the LDH precursor. The crystal structure of this material was determined by Rietveld refinement of an isostructural ammonium nickel molybdate. The structure is trigonal, with hexagonal unit-cell parameters of $a = 6.10767(15)$ Å and $c = 21.6409(6)$ Å. The host structure consists of divalent cation octahedra which share edges to form layers perpendicular to the c axis, analogous to the LDH precursor. The tetrahedral molybdate species, however, are not merely intercalated within the interlayer domain but are bonded to the layers themselves through shared Mo−O−Zn bonds. This arrangement results in the formation of a net negative charge on the host structure, leading to incorporation of ammonium ions between the layers for charge balancing. The applicability of this novel synthesis route is dependent on the composition of the original LDH, and it appears that metastability in the calcined LDH favors conversion to this phase.

Introduction

Pillared layered structures (PLS) are nanocomposite materials prepared by linking molecules to a layered host. These structures are an excellent example of materials by design. Synthesis of these PLS can be accomplished by modification of the host−structure chemical composition, chemical or structural modification of the interlayer region, or both. There has been extensive research into the preparation of PLS, focused mainly on structural modification of the interlayer region. Examples include the pillaring of smectites, such as montmorillonite, by ion-exchange with polycationic species, e.g., Al_{13}−polyhydroxy polymer $(Al_{13}O_4(OH)_{24}(H_2O)_{12})^{7+}$,[1−6] Zr−hydroxy polymers $(Zr_4(OH)_8(H_2O)_{16})^{8+}$,[7,8] and other oligocations. One common feature of these materials, termed cross-linked smectite (CLS) molecular sieves, or pillared interlayered clays (PILC), is that they are prepared without chemical modification of the host composition. Other examples of PLS prepared by modification of only the interlayer region include the pillaring of layered double hydroxides (LDHs), also known as hydrotalcite-like materials, by various anionic species. Examples include the pillaring of LDHs with polyoxometalate (POM) anions of the $[XM_{12}O_{40}]^{m-}$ or Keggin ion type by direct anion exchange,[9−14] or utilizing an organic anion-pillared precursor that was subsequently exchanged with the appropriate isopolymetalate under mildly acidic conditions.[15,16] To the best of our knowledge, however, no new layered structure has been prepared by the simultaneous modification of both the chemical composition of the host structure and the interlayer region. In this paper, we report a novel room-temperature *chimie douce* synthesis technique that produced a new class of layered transition-metal molybdate (LTM) materials using calcined LDHs as precursors. These new materials, while being related structurally to the original LDH, have undergone a modification of the host chemical composition with complete transformation of the interlayer region.

Structure of LDH Precursor

Layered double hydroxides (LDHs) or the so-called anionic clays are, in terms of charge, mirror images of the extensively studied family of cationic smectite clay minerals. The structure, synthesis, and properties of these materials have been extensively reviewed.[17]

† Massachusetts Institute of Technology.
‡ Exxon Research and Engineering Company.
* To whom correspondence should be addressed.
⊗ Abstract published in *Advance ACS Abstracts,* March 1, 1996.

(1) Brindley, G. W.; Sempels, R. E. *Clay Miner.* **1977**, *12*, 229.
(2) Lahav, N.; Shani, U.; Shabti, J. *Clays Clay Miner.* **1978**, *26*, 107.
(3) Pinnavaia, T. J.; Tzou, M.-S.; Landau, S. D.; Raythatha, R. H. *J. Mol. Catal.* **1984**, *27*, 195.
(4) Occelli, M. L.; Tindwa, R. M. *Clays Clay Miner.* **1983**, *31*, 22.
(5) Tokarz, M.; Shabtai, J. *Clays Clay Miner.* **1985**, *33*, 89.
(6) Schutz, A.; Stone, W. E. E.; Poncelet, G.; Fripiat, J. J. *Clays Clay Miner.* **1987**, *35*, 251.
(7) Jones, S. L. *Catal. Today* **1988**, *2*, 209.
(8) Sterte, J. *Catal. Today* **1988**, *2*, 219.
(9) Kwon, T.; Tsigdinos, G. A.; Pinnavaia, T. J. *J. Am. Chem. Soc.* **1988**, *110*, 3653.
(10) Kwon, T.; Pinnavaia, T. J. *Chem. Mater.* **1989**, *1*, 381.
(11) Doeuff, M.; Kwon, T.; Pinnavaia, T. J. *Synth. Met.* **1989**, *34*, 609.
(12) Kwon, T.; Pinnavaia, T. J. *J. Mol. Catal.* **1992**, *74*, 23.
(13) Wang, J.; Tian, Y.; Wang, R.-C.; Colón, J. L.; Clearfield, A. *Mater. Res. Soc. Symp. Proc.* **1991**, *233*, 63.
(14) Wang, J.; Tian, Y.; Wang R.-C; Clearfield, A. *Chem. Mater.* **1992**, *4*, 1276.
(15) Drezdzon, M. A. U.S. Patent 4,774,212, 1988.
(16) Drezdzon, M. A. *Inorg. Chem.* **1988**, *27*, 4628.
(17) Cavani, F.; Trifirò, F.; Vaccari, A. *Catal. Today* **1991**, *11*, 173.

0897-4756/96/2808-0836$12.00/0

The structure of LDHs, shown schematically in Figure 1, is very similar to that of brucite, $Mg(OH)_2$, where octahedra of Mg^{2+} (6-fold coordinated to OH^-) share edges to form infinite sheets. These sheets are stacked on top of each other and are held together by hydrogen bonding. Isomorphous substitution of a divalent cation in the lattice by a trivalent cation having similar radius results in a positive charge generated in the hydroxy sheet. This net positive charge is compensated for by incorporation of hydrated anions in the interlayer region.

The composition of LDHs is typically represented by the general formula

$$[M^{II}_{1-x}M^{III}_{x}(OH)_2]^{x+}[A^{n-}_{x/n}\cdot zH_2O]$$

where A^{n-} is the gallery anion and M^{II} and M^{III} are the divalent and trivalent cations, respectively. Typically M^{II} may be Mg^{2+}, Zn^{2+}, Ni^{2+}, Co^{2+}, or Fe^{2+}, and M^{III} may be Al^{3+}, Cr^{3+}, Co^{3+}, or Fe^{3+}. There is essentially no limitation to the nature of the anion and A^{n-} is typically CO_3^{2-}, NO_3^-, OH^-, or Cl^-. Many compositions are possible, depending on the combination of M^{II}, M^{III}, A^{n-}, and the layer cation stoichiometry. Typically, the trivalent cation substitution parameter, x, given by $M^{III}/(M^{II} + M^{III})$, is in the range 0.17−0.33.

LDHs crystallize in either the $R\bar{3}m$ space group (rhombohedral phase) or the $P6_3/mmc$ space group (hexagonal phase). In the rhombohedral phase, three double layers are present per unit cell, resulting in the hydroxyl stacking sequence *BC*−*CA*−*AB*−*BC* (where *A*, *B*, and *C* are the three 3-fold axes at $x, y = 0,0$; $^2/_3,^1/_3$; and $^1/_3,^2/_3$).[18] In the hexagonal phase, only two double layers are present per unit cell, leading to a hydroxyl stacking sequence *BC*−*CB*−*BC*. Only the three-layered rhombohedral phase is known for synthetic LDHs formed by coprecipitation from aqueous media.

Thermal Decomposition of Layered Double Hydroxide Precursor

The thermodynamically stable products of calcination of a $M^{II}M^{III}$−LDH in an inert gas are a spinel $M^{II}M^{III}_2O_4$ and free $M^{II}O$. At temperatures between initial LDH decomposition and spinel phase formation, a series of metastable phases, both crystalline and amorphous, form.[19] The properties of these phases depend on the cations constituting the original LDH, preparation and thermal decomposition conditions, and the presence of impurities.[17]

The process of thermal decomposition of a carbonate LDH consists of dehydration, represented by the formula

$$[M^{II}_{1-x}M^{III}_{x}(OH)_2]^{x+}[(x/2)CO_3^{2-}\cdot zH_2O] \rightarrow [M^{II}_{1-x}M^{III}_{x}(OH)_2]^{x+}[(x/2)CO_3^{2-}] + zH_2O \quad (1)$$

followed by dehydroxylation and decarbonation, yielding a mixed oxide phase at temperatures less than 550 °C, given by

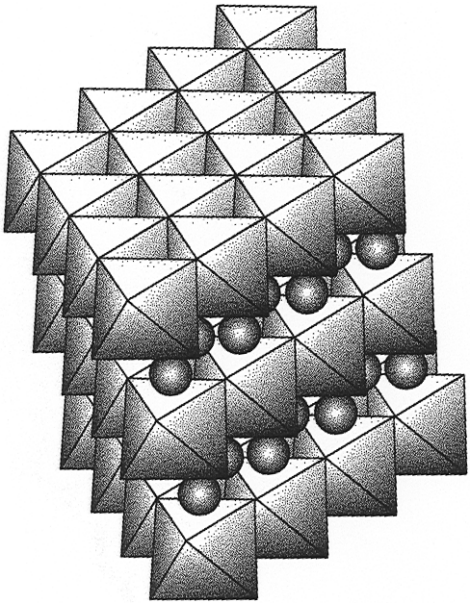

Figure 1. Schematic representation of LDH.

$$[M^{II}_{1-x}M^{III}_{x}(OH)_2]^{x+}[(x/2)CO_3^{2-}] \rightarrow M^{II}_{1-x}M^{III}_{x}O_{1+x/2} + (x/2)CO_2 + H_2O \quad (2)$$

Reconstitution of Layered Double Hydroxides: "Memory Effect"

The term "memory effect" describes the capacity of samples prepared by thermal decomposition of LDH precursors containing a volatile anion such as carbonate to reconstitute the original layered structure upon adsorption of various anions[20] or simply upon exposure to air.[21] This process can be represented by the formula

$$M^{II}_{1-x}M^{III}_{x}O_{1+x/2} + (x/m)B^{m-} + (1 + x/2)H_2O \rightarrow [M^{II}_{1-x}M^{III}_{x}(OH)_2]^{x+}[(x/m)B^{m-}] + xOH^- \quad (3)$$

The reconstitution behavior is governed by the electrostatic interaction between the positively charged host layer and the interlayer anions. Since the rehydrolysis process generates OH^- ions, the degree of uptake will be governed by the anion exchange equilibrium between B^{m-} and OH^- for the LDH. As suggested by the reconstitution reaction 3, the pH of the reacting solution should increase with the progress of the reaction.

This reconstitution process has been used as a method for altering the composition of a LDH. By thermally decomposing an easily synthesized carbonate form of LDH to a mixed oxide phase and then exposing the latter to an aqueous solution, a desirable anion, B^{m-}, could be intercalated. Using this method, isopolyoxometalates such as $V_{10}O_{28}^{6-}$ and $Mo_7O_{24}^{6-}$ anions had been incorporated into a LDH structure upon reconstitution.[22−24] This technique had also been used to incorporate certain dicarboxylic acid dianions.[25] How-

(18) Allmann, R. *Acta Crystallogr.* **1968**, *B24*, 972.
(19) Puxley, D. C.; Kitchener, I. J.; Komodromos, C.; Parkyns, N. D. *Preparation of Catalysts III*; Poncelet, G., Grange, P., Jacobs, P. A., Eds.; Elsevier Science: Amsterdam, 1983; p 237.
(20) Sato, T.; Wakabayashi, T.; Shimada, M. *Ind. Eng. Chem. Prod. Res. Dev.* **1986**, *25*, 89.
(21) Rey, F.; Fornés, V.; Rojo, J. M. *J. Chem. Soc., Faraday Trans.* **1992**, *88*, 2233.
(22) Chibwe, K.; Jones, W. *Chem. Mater.* **1989**, *1*, 489.
(23) Misra, C.; Perotta, A. J. U.S. Patent 5,075,089, 1991.
(24) Narita, E.; Kaviratna, P.; Pinnavaia, T. J. *Chem. Lett.* **1991**, 805.
(25) Chibwe, K.; Jones, W. *J. Chem. Soc., Chem. Commun.* **1989**, 926.

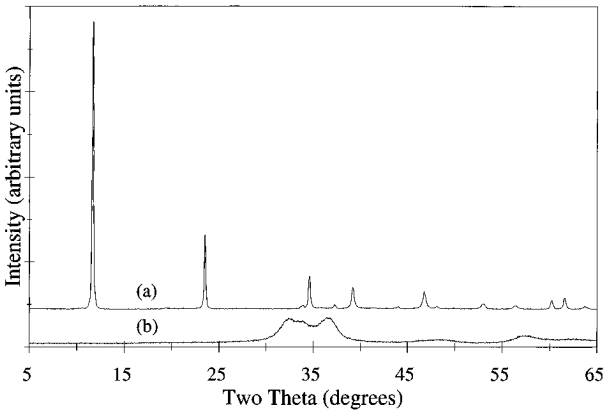

Figure 2. Powder X-ray diffraction pattern of (a) $Zn_4Al_2(OH)_{12}CO_3{\cdot}4H_2O$ and (b) the calcined LDH precursor.

ever, despite literature claims to the contrary,[24] the reconstitution reaction 3 is *not* general but depends significantly on the composition of the metastable mixed oxide phase and the nature of the anion B^{m-}. The countercation, C^{q+}, present from the salt from which B^{m-} is derived, can also be involved in the reaction of the metastable mixed oxide. Perturbing the metastable oxide by exposing it to an aqueous solution of specific B^{m-} and C^{q+} ions can lead to reactions producing new, highly crystalline phases. In this paper, the reaction between a Zn/Al mixed oxide and ammonium and molybdate ions that produced a layered ammonium zinc molybdate termed Zn−LTM is presented.

Experimental Section

The overall synthesis route of the Zn−LTM can be represented as follows:

$$\text{Zn,Al salts} \xrightarrow{\text{precipitation}} \text{Zn/Al−LDH} \xrightarrow{\text{calcination}} \text{Zn/Al mixed oxide} \xrightarrow{\textit{chimie douce}\text{ reaction}} \text{Zn−LTM}$$

Preparation of the Metastable Mixed Oxide Precursor. The mixed oxide precursor for the synthesis of Zn−LTM was derived from $Zn_4Al_2(OH)_{12}CO_3{\cdot}zH_2O$ LDH. The LDH was synthesized by coprecipitation at constant pH, under conditions of low supersaturation. The precursor was prepared by adding a solution of $Zn(NO_3)_2{\cdot}6H_2O$ and $Al(NO_3)_3{\cdot}9H_2O$ to a solution of KOH and K_2CO_3, at relative rates such that a constant pH of 9.0 was maintained. The temperature of precipitation was 55 ± 2 °C. Following precipitation, the material was aged in the mother liquor overnight at 70 °C. The material was then filtered, washed, and dried at 110 °C and at atmospheric pressure. The X-ray diffraction pattern of this material, shown in Figure 2a, has sharp and symmetrical peaks characteristic of a well-crystallized Zn/Al−LDH.[26] The pattern was indexed in rhombohedral symmetry on hexagonal axes with a = 3.06(5) Å and c = 22.65(5) Å, determined by a least-squares method. The X-ray diffraction analysis confirmed the absence of a secondary zincite (ZnO) phase. The single phase LDH was expected as x = Al/(Zn + Al) = 0.33 was in the range 0.3−0.4 in which single-phase Zn/Al LDHs form.[26]

The Zn_4Al_2−LDH was calcined in air at 500 °C for 3.5 h. The X-ray diffraction pattern of the calcined precursor is shown in Figure 2b. The broad peaks are in positions similar to those of ZnO (zincite), which allowed for the indexing of the peaks on a hexagonal unit cell. A least-squares procedure was used to estimate the lattice constants from the 100, 101, 110, and 112 peak positions. The lattice constants of the calcined LDH

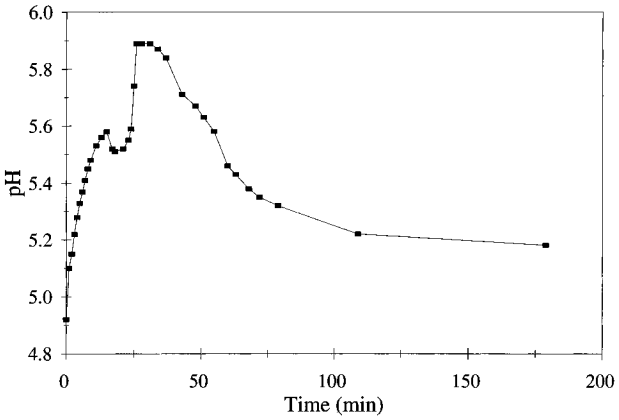

Figure 3. Change in pH during *chimie douce* reaction.

(a = 3.21(3) Å, c = 5.12(3) Å) are smaller than those of pure ZnO (a = 3.24982(9) Å, and c = 5.20661(15) Å (PDF Card 36−1451)), which led to the conclusion that the calcined LDH was a poorly crystalline Zn/Al solid solution conforming to the zincite lattice structure.

***Chimie Douce* Synthesis of Zn−LTM.** The Zn−LTM phase was synthesized by adding the metastable mixed oxide to a room-temperature solution of ammonium heptamolybdate (0.05 M $Mo_7O_{24}^{6-}$ and 0.3 M NH_4^+). Progress of the reaction was followed by monitoring the pH. A typical pH profile over the course of the reaction is shown in Figure 3. The pH profile indicates the complexity of the solution chemistry occurring during the *chimie douce* reaction. The variation in the pH reflects a complex competition between the generation and consumption of hydroxyl ions. Increases in pH result from the generation of hydroxyl ions by rehydrolysis of the zinc oxide and reaction of the hydrolyzed dealuminated defect zinc oxide with molybdate anions. Hydroxyl ions are consumed by the reactions

$$Mo_7O_{24}^{6-} + 8OH^- \rightarrow 7MoO_4^{2-} + 4H_2O \quad (4)$$

$$mAl^{3+} + nOH^- \rightleftarrows Al_m(OH)_n^{(3m-n)+} \quad (5)$$

leading to a lowering of the pH. The *chimie douce* reaction was deemed complete after observation of a constant pH. Following completion of the reaction, the product was recovered by filtration, washed with deionized water, and dried overnight at 110 °C. The product, called Zn−LTM, was a fine white powder.

Characterization of Zn−LTM. Elemental analysis of the LDH and the Zn−LTM was determined by X-ray fluorescence (Oneida Research Services). The Zn and Al content of the Zn_4Al_2−LDH was 41.2 and 8.02 wt % respectively, giving a Zn/Al molar ratio of 2.1. Following *chimie douce* reaction with ammonium heptamolybdate solution, the Zn−LTM product analyzed as 33.8 wt % Mo, 0.63 wt % Al, and 24.6 wt % Zn. The Zn/Mo and Zn/Al molar ratios in the product were therefore 1.07 and 16.1, respectively. There was thus an almost 8-fold increase in the Zn/Al ratio, resulting from Al leaving the solid on reaction with the ammonium heptamolybdate solution. The loss of Al from the structure led to the designation of this compound as Zn−LTM, as opposed to Zn-Al−LTM.

The photoacoustic Fourier transform infrared (PA-FTIR) spectrum of the Zn−LTM is shown in Figure 4. This spectrum was collected with a 2.5 kHz rapid scan at 8 cm^{-1} resolution, using a MTEC Model 200 photoacoustic cell in a BioRad FTS-60A spectrometer. The PA-FTIR spectrum confirmed the presence of NH_4^+ ions in the structure, as evidenced by the ν_3(N−H) asymmetric stretch in the region 3300−3050 cm^{-1} and the ν_4(H−N−H) deformation at 1408 cm^{-1}.[27] The spectrum also shows the presence of an overtone at 2820 cm^{-1} ($2\nu_4$) and a combination band at 3040 cm^{-1} ($\nu_2 + \nu_4$).[27] The

(26) Thevenot, F.; Szymanski, R.; Chaumette, P. *Clays Clay Miner.* **1989**, *37*, 396.

(27) Waddington, T. C. *J. Chem. Soc.* **1958**, 4340.

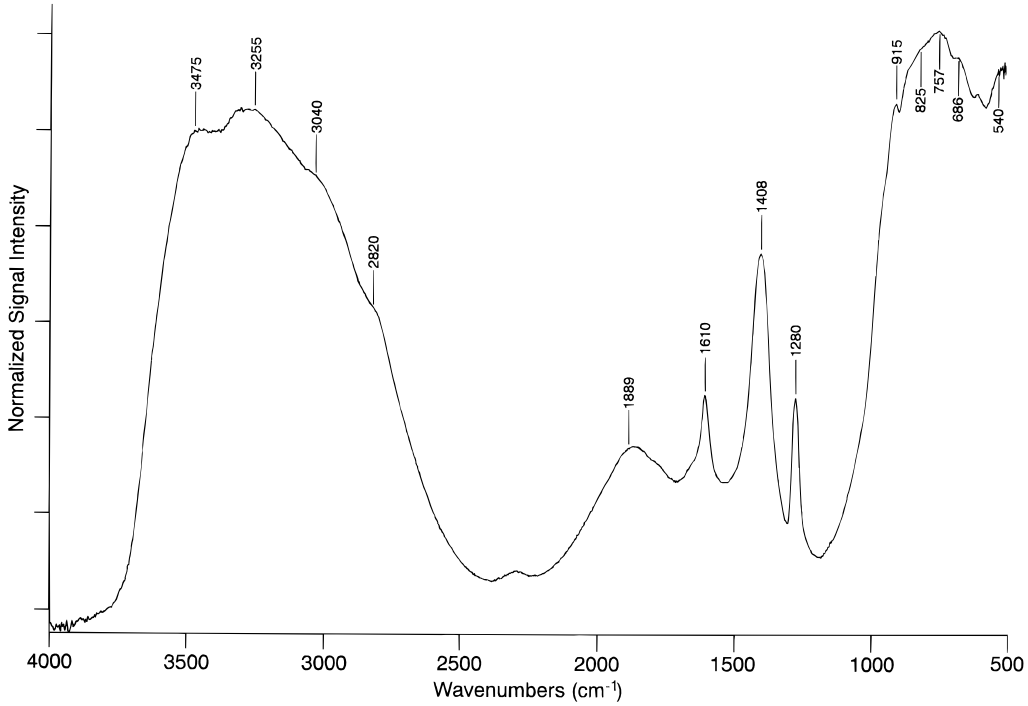

Figure 4. PA-FTIR spectrum of Zn−LTM.

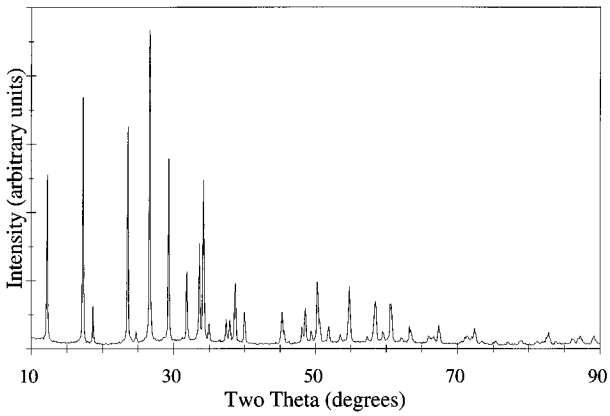

Figure 5. Powder X-ray diffraction pattern of Zn−LTM.

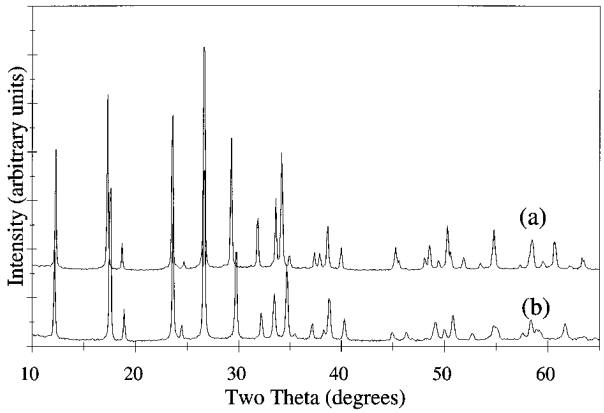

Figure 6. X-ray diffraction patterns of (a) Zn−LTM and (b) $(NH_4)HNi_2(OH)_2(MoO_4)_2$, showing isostructural relationship.

broad band in the region 1600−2000 cm^{-1} arises from the interaction of ν_4 with the torsional oscillation ν_6 of the ammonium on its lattice site,[27] suggesting that the ammonium ion is not freely rotating. The PA-FTIR characterization proved that repeated washing of the material had failed to remove the ammonium ions, leading to the conclusion that the ammonium ions were a part of the crystal structure.

A powder X-ray diffraction pattern of this material, collected on a Siemens D5000 θ/θ diffractometer operated at 45 kV and 40 mA with Cu Kα radiation, is shown in Figure 5. A step-scanned diffraction pattern was collected from 10 to 90° 2θ (0.02° step, 2.5 s/step, sum of three scans) for use in Rietveld refinement of the structure. This diffraction pattern is significantly different from ZnO and bears no resemblance to that expected from a LDH pillared with the heptamolybdate anion.[22,23] A search of the JCPDS database found an almost identical match with a phase belonging to a family of ammonium−divalent cation−molybdenum oxides reported by French workers[28] (PDF Card 40-674). As an example of this phase, an ammonium nickel molybdate compound had been prepared by direct precipitation from a solution of nickel nitrate and ammonium heptamolybdate, a route that did not involve LDH precursors. The X-ray diffraction patterns of Zn−LTM and this ammonium nickel molybdate (Figure 6a,b, respectively) clearly show that the two phases are isostructural. The knowledge of the crystal structure of one of these phases would obviously allow for rapid refinement of the other.

The crystal structure of the nickel analogue prepared by precipitation was solved first. The reason for choosing the nickel analogue in preference to the Zn−LTM phase was the fact that the nickel analogue only contained a single divalent cation (Ni), while the Zn−LTM phase seemed to contain both Al^{3+} and Zn^{2+}, in a ratio that differed significantly from the LDH precursor. The *ab initio* crystal structure determination of the ammonium nickel molybdate analogue was accomplished using a combination of three-dimensional Patterson methods, difference Fourier syntheses, and Rietveld refinement of synchrotron X-ray powder diffraction data.[29] This solution of the crystal structure was, however, facilitated by the knowledge that an isostructural analogue could be prepared from a LDH precursor. This had suggested $R\bar{3}m$ as the probable space group, in analogy to the rhombohedral LDH. In addition, the lattice parameters of the Zn−LTM seemed related to those of the LDH precursor. The XRD patterns of the Zn−LTM shown in Figure 5 and of the Zn-Al LDH shown in Figure 2a were indexed in a rhombohedral cell on hexagonal axes. For the Zn−LTM, $a \approx 2a_0$ and $c \approx c_0 - 1$Å, where a_0

(28) Astier, M. P.; Dji, G.; Teichner, S. J. *Ann. Chim. Fr.* **1987**, *12*, 337.

(29) Levin, D.; Soled, S. L.; Ying, J. Y. *Inorg. Chem.*, submitted.

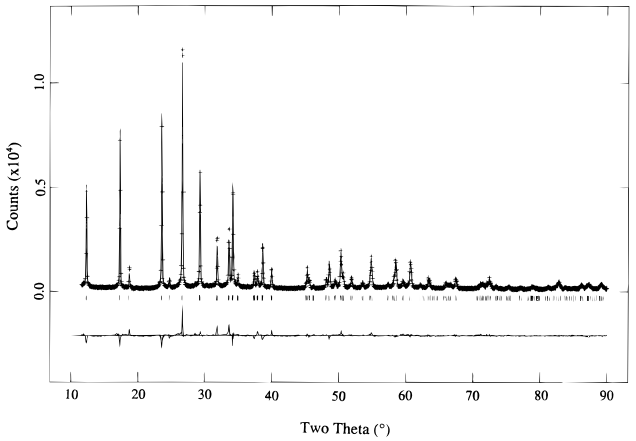

Figure 7. Powder X-ray data, including Rietveld fit and residuals for Zn−LTM. In the upper field, points shown as + represent observed data, and the continuous line is the calculated profile from the refinement. The difference pattern, observed minus calculated profiles, is shown in the lower field. The set of short vertical bars below the data set indicate the position of possible Bragg reflections.

Table 1. Final Positional and Thermal Parameters

atom	Wyckoff	x	y	z	$100U_{iso}$	fraction
Mo	6(c)	0	0	0.09229(8)	*a*	1.0
Zn	9(e)	1/2	0	0	2.06(13)	0.642(4)
O(1)	6(c)	0	0	0.2996(4)	1.83(32)	1.0
O(2)	6(c)	0	0	0.1719(6)	7.37(48)	1.0
O(3)	18(h)	0.3137 (10)	0.1568 (5)	−0.06476 (24)	4.40(24)	1.0
N	3(b)	0	0	1/2	0.5(0)[b]	1.0

[a] $100(U_{11} = U_{22}) = 2.91(8)$, $100U_{33} = 0.76(8)$, $100U_{12} = 1.45(4)$, $U_{13} = U_{23} = 0$. [b] Not refined.

and c_0 are the lattice parameters of the original LDH, suggesting that the Zn−LTM could be a supercell of a modified LDH. It was, however, surprising that *c* was less than expected, suggesting that the Zn−LTM structure was not accommodating the heptamolybdate anion in an arrangement analogous to that of carbonate in the LDH. This hypothesis was confirmed after completion of the structure determination of the nickel analogue which showed molybdate tetrahedra actually bonded to the nickel hydroxy sheets.[29] Knowledge of the crystal structure of the ammonium nickel molybdate analogue, $(NH_4)HNi_2(OH)_2(MoO_4)_2$, allowed for the rapid refinement of the structure of the Zn−LTM. Rietveld refinements were performed using General Structure Analysis System, GSAS.[30]

Solution and Refinement of the Zn−LTM Structure. The crystal structure was refined by the Rietveld method, using the structure of an isostructural nickel analogue, $(NH_4)HNi_2(OH)_2(MoO_4)_2$,[29] as a starting model. The refinement converged with $R_{wp} = 9.8\%$ and $R_p = 7.9\%$. The data, fit, and residuals are shown in Figure 7. The atomic positions and thermal parameters are listed Table 1, and the summary of the refinement is given in Table 2. The refinement included background, lattice parameters, the Gaussian profile, the Lorentzian profile, asymmetry, atom positions, and thermal parameters. Isotropic temperature parameters were used for all atoms except molybdenum.

In an attempt to account for the small percentage of Al reported by chemical analysis, Al atoms were placed on the same 9(e) site as Zn. When the fractional occupancy for the Al was set on the basis of the elemental analysis, the thermal parameter for Al increased immediately to 0.400, the maximum that GSAS will allow, after a few cycles of refinement. Alternatively, when the thermal parameter of the Al was constrained to equal that of the Zn, and the fractional occupancy was allowed to vary, the occupancy refined to zero. This led to the conclusion that the Al is not actually in the structure itself but is probably present as a small amorphous phase. This assumption is supported by the relatively high number of terms (12) required to fit the background satisfactorily.

(30) GSAS, General Structure Analysis System, Larson, A. C.; von Dreele, R. B., LANSCE, Los Alamos National Laboratory, copyright 1985−1994 by the Regents of the University of California.

Table 2. Crystallographic Data for $(NH_4)HZn_2(OH)_2(MoO_4)_2$ from Rietveld Refinement of Powder X-ray Diffraction Data

powder color	white
formula	$(NH_4)HZn_2(OH)_2(MoO_4)_2$
formula weight (g/mol)	498.9
space group	$R\bar{3}m$
a (Å)	6.10767(15)
c (Å)	21.6409(6)
V (Å^3)	699.13(4)
Z	3
D_{calc} (g/cm^3)	3.56
background: cosine Fourier series	12 terms
R_{wp}	9.8%
R_p	7.9%
R_F	9.6%
R_{exp}	5.2%

Hydrogen positions were assigned on the basis of difference Fourier maps, as discussed in the crystal structure solution of the isostructural nickel analogue.[29] This assignment of protons led to the chemical formula for the Zn−LTM compound of $(NH_4)HZn_2(OH)_2(MoO_4)_2$. After completion of the structure determination, we discovered the crystal structure of the Zn−LTM and its chemical formula to be in agreement with an incomplete single-crystal study of a zinc molybdate phase designated in the literature by Pezerat[31] as Φ_y and given the "ideal" formula $H_3(NH_4)Zn_2Mo_2O_{10}$.

Crystal Structure of Zn−LTM

The framework of Zn−LTM consists of sheets of distorted zinc octahedra to which tetrahedral molybdate groups are bonded. These layers are stacked in the *c* direction and are held together by hydrogen bonding. The zinc atoms defining these layers are located at site 9(e), which can vary in occupancy from $^1/_2$ to 1.[29] If the occupancy of this site is one, the arrangement of zinc atoms can be considered as a pattern of two alternating strings, one being Zn−Zn−Zn, as in LDH, the other being Zn−□−Zn, where □ represents an ordered cation vacancy. This ordered cation vacancy is independent of the zinc occupancy. As the zinc occupancy deviates from unity, additional disordered vacancies appear in the sheet. For the Zn−LTM, having a zinc occupancy of $^2/_3$, three of every nine zinc sites are vacant. The coordination of oxygens about the zinc atoms is distorted octahedral, with a tetragonal contraction along the C_4 axis running through O(1)−Zn−O(1). The bond distances and angles defining the distorted octahedra are shown in Tables 3 and 4. The zinc atoms are linked to each other through double hydroxyl bridges. Each zinc octahedron shares edges with a maximum of four adjacent octahedra, thereby creating the sheets of octahedra perpendicular to the *c* axis.

The absence of a zinc atom at the origin generates ordered vacancies in the sheet. These vacant octahedral sites are capped, both above and below, by tetrahedral molybdate groups. Disordered vacant octahedral sites resulting from a reduction in the zinc occupancy from unity are, however, not capped by tetrahedral molybdate groups. The molybdate tetrahedra above and below an

(31) Pezerat, H. *Bull. Soc. Fr. Miner. Cristallogr.* **1967**, *90*, 549.

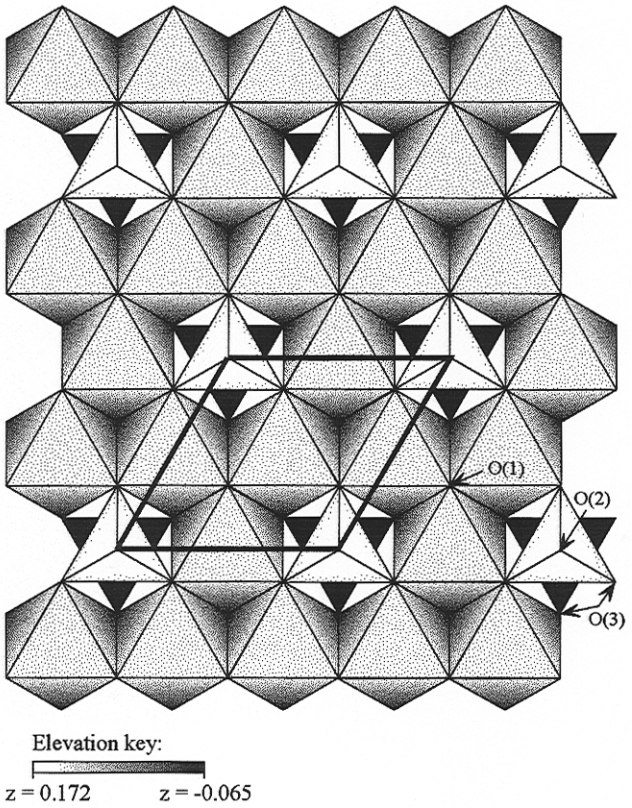

Figure 8. Basal plane of Zn−LTM, viewed along [001].

Table 3. Selected Interatomic Distances

atom pair	distance (Å)
bonded	
Mo−O(2)	1.722(12)
Mo−O(3) (×3)	1.763(5)
Zn−O(1) (×2)	1.908(4)
Zn−O(3) (×4)	2.295(5)
nonbonded	
Mo−Mo (across layer)	3.992(8)
Zn−Zn (between adjacent layers)	7.213(6)
O(2)−O(1)	2.764(6)
N−O(1)	4.337(6)
N−O(2)	3.528(6)
N−O(3)	2.889(5)

Table 4. Selected Interatomic Angles

atoms	angle (deg)
O(2)−Mo−O(3) (×3)	109.75(18)
O(3)−Mo−O(3) (×3)	109.19(18)
Zn−O(1)−Zn (×3)	106.28(2)

ordered vacancy are related to each other by the center of inversion at the origin. The tetrahedra share three of their corners with the zinc−oxygen octahedra at O(3). Since there are four O(3) atoms in each octahedron, four octahedral corners are shared with four different molybdate tetrahedra. Each molybdate tetrahedron shares corners with six different zinc octahedra, generating the hexagonal arrangement shown in Figure 8.

The three zinc molybdate layers defining the unit cell are stacked at a separation of $c/3 = 7.2136(6)$ Å. In these layers, the position of the ordered vacant octahedral site capped by the molybdate groups follows the sequence $A-B-C-A$ (where A, B, and C are the three 3-fold axes at $x, y = 0,0$; $^2/_3,^1/_3$; and $^1/_3,^2/_3$). This three-layer arrangement is shown in Figure 9. Between each layer, in the octahedral space defined by O(3) oxygens of six tetrahedral molybdates, lie ammonium ions. The

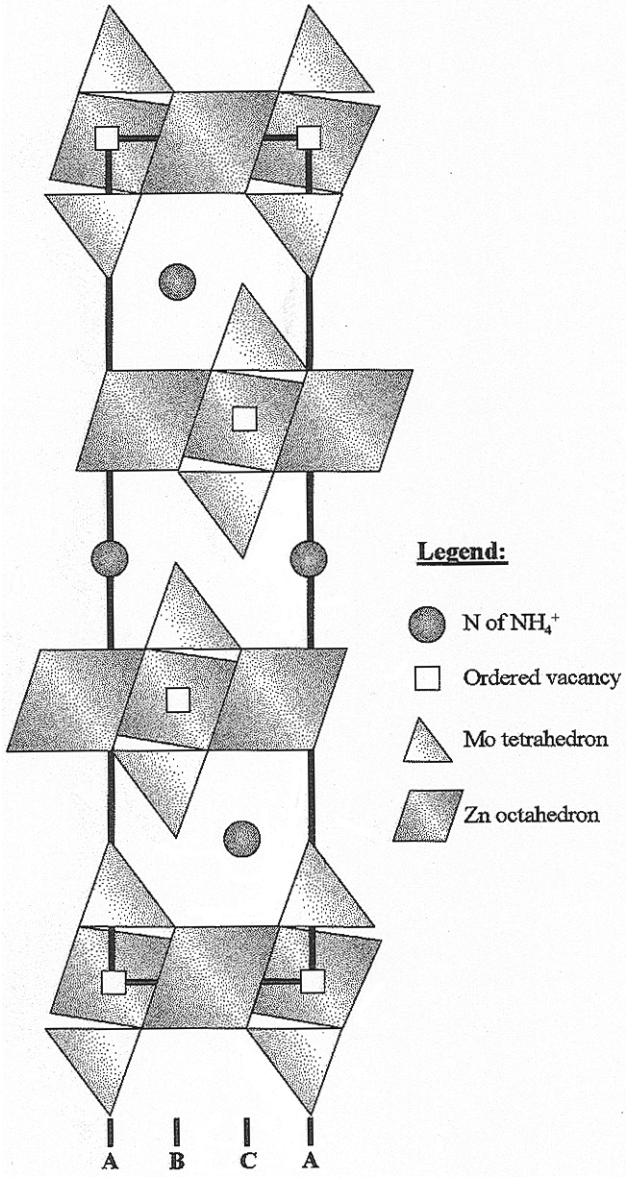

Figure 9. Crystal structure of Zn−LTM, viewed along [010], showing three-layer arrangement in polyhedron representation.

positions of the nitrogen atoms follow the sequence $C-A-B-C$. The N−O(3) distance of 2.89 Å suggests that the ammonium ions are oriented with three of the four hydrogens directed toward O(3), thereby anchoring the ammonium ion via a hydrogen-bonding mechanism. The arrangement of O(3) atoms is symmetrically equivalent above and below the nitrogen, suggesting that two orientations for the ammonium ions are possible. The ammonium ions can likely be found in either orientation with equal probability. The restriction on the orientation of the ammonium ions is supported by the infrared spectroscopic analysis that suggested that the ammonium ions are not freely rotating. The ammonium ions, however, do not serve to connect the array of layers in the [00l] direction, the N−O(1) distance of 4.34 Å being too long for hydrogen bonding. The vertical distance between O(2), the apical oxygen of the molybdate tetrahedra, and O(1), the bridging oxygen of the adjacent zinc layer, is 2.76 Å, suggesting that these two oxygens are involved in a hydrogen bonding mechanism that serves to connect the layers. Figure 10 illustrates

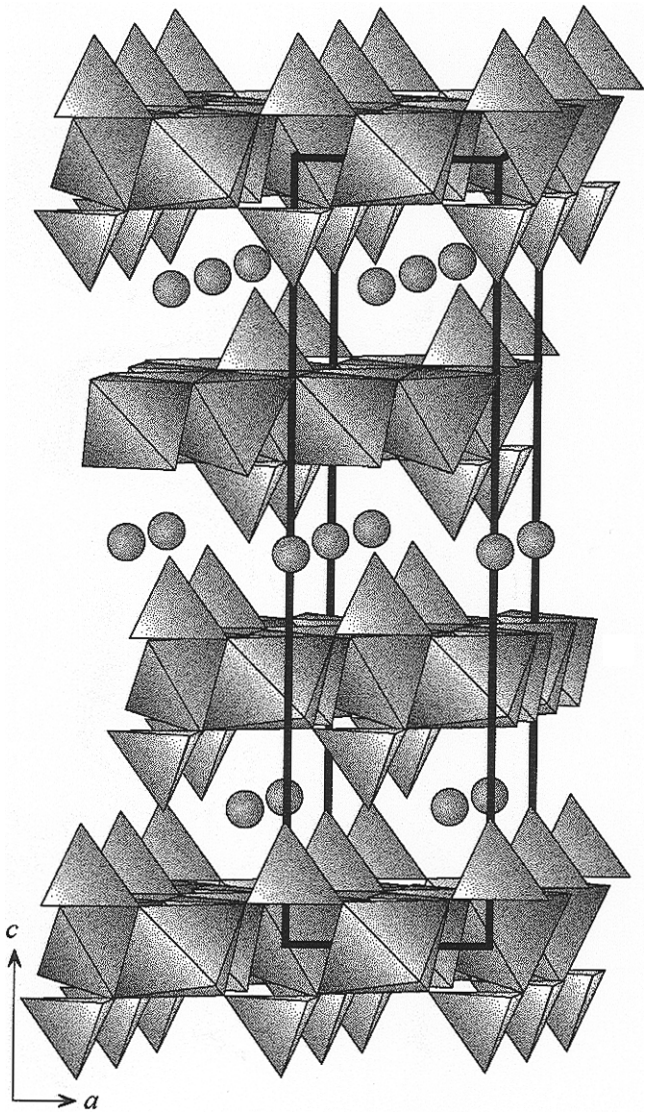

Figure 10. Crystal structure of Zn−LTM, viewed in polyhedron representation.

a three-dimensional polyhedron representation of the crystal structure of Zn−LTM.

Discussion

The *chimie douce* reaction with ammonium heptamolybdate solutions occurred only with mixed oxide phases derived from LDHs of the form $[Zn_{(1-x-y)}M^{II}_yAl_x(OH)_2]^{x+}$-$[(CO_3)_{x/2}\cdot zH_2O]$, where M^{II} was Cu^{2+}, Co^{2+}, and Ni^{2+}, and $(1 - x - y)/x > 1$. This suggests a general formula for Zn−LTM as $(NH_4)HZn_{2-w}M^{II}_w(OH)_2(MoO_4)_2$, where $M^{II} = Cu^{2+}$, Co^{2+}, or Ni^{2+}, and $w < 1$. No *chimie douce* reaction with ammonium heptamolybdate solutions occurred for mixed oxide phases prepared from $[M^{II}_{1-x}$-$Al_x(OH)_2]^{x+}[(CO_3)_{x/2}\cdot zH_2O]$ precursors, where $M^{II} = Mg^{2+}$ or Ni^{2+} (i.e., any M^{II} whose corresponding oxide, $M^{II}O$, is of the rock-salt structure). In the latter case, the heptamolybdate anion is pillared between the reconstituted LDH[21,22] without forming the LTM crystalline phase.

To investigate the reason for the reactivity of the aluminum-substituted oxide phases, samples of Zn_4-$Al_2(OH)_{12}CO_3\cdot zH_2O$ and $Mg_4Al_2(OH)_{12}CO_3\cdot zH_2O$ were calcined at 500 °C for 3.5 h in air, allowed to cool in a desiccator, and then examined by ^{27}Al magic angle spinning nuclear magnetic resonance (MAS NMR) spectroscopy. Solid-state aluminum NMR spectra were acquired at room temperature with magic angle spinning on a Chemagnetics CMX-500 operating at 130.27 MHz. Samples were typically spun at frequencies of 6 kHz, and the spectra were referenced to aqueous solutions of aluminum sulfate (resonance frequency = 0 ppm). The NMR spectra of the Al-substituted ZnO phase and the Al-substituted MgO phase are shown in Figure 11a,b, respectively. The peak around 0 ppm is attributed to octahedrally coordinated aluminum, Al_O, and the peak around 65−70 ppm is attributed to tetrahedrally coordinated aluminum, Al_T.[32] Comparing integrated peak intensities, the Al_T/Al_O ratios were determined to be 5.25 for the calcined Zn_4Al_2−LDH and 0.75 for the calcined Mg_4Al_2−LDH. The result for the Al_T/Al_O ratio for the calcined Mg_4Al_2−LDH is in agreement with a value of 0.70 reported in the literature.[33] These results seem to indicate that a very high proportion of tetrahedrally coordinated Al is a requisite for the *chimie douce* reaction producing the LTM phase.

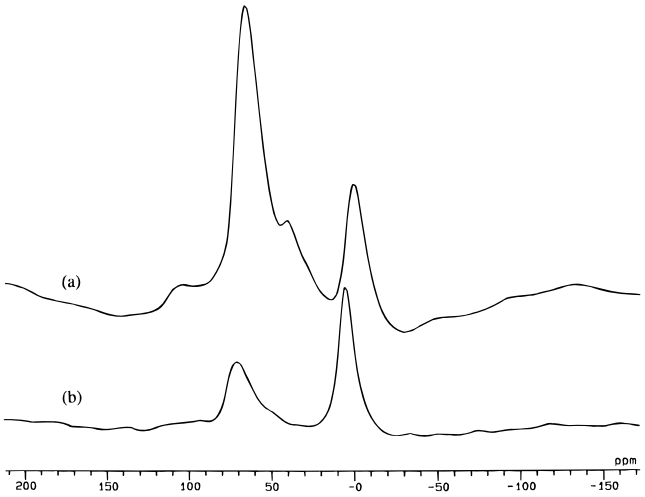

Figure 11. ^{27}Al NMR spectra of (a) calcined $Zn_4Al_2(OH)_{12}$-$CO_3\cdot 4H_2O$ and (b) calcined $Mg_4Al_2(OH)_{12}CO_3\cdot 4H_2O$.

It is interesting to compare the fraction of tetrahedrally coordinated aluminum in the calcined Al-substituted ZnO phase to the Al content of Zn−LTM powder, as determined by chemical analysis. Using integrated peaks intensities of the NMR data shown in Figure 11a, the percentage of tetrahedrally coordinated aluminum was found to be 84%. If, assuming that all tetrahedrally coordinated aluminum and none of the octahedrally coordinated aluminum enter into solution on *chimie douce* reaction, there will be a reduction in the cation content from a Zn_4Al_2 precursor to a $Zn_4Al_{0.32}$ product, resulting in a Zn/Al ratio of 12.5. The Zn/Al ratio determined by chemical analysis was 16.1. Since accurate determination of a true Al_T percentage in the sample is complicated by asymmetric line broadening from secondary quadrupolar effects, there is sufficiently reasonable agreement between the NMR and chemical analyses to suggest that the *chimie douce* reaction proceeds via loss of tetrahedrally coordinated aluminum from the metastable mixed oxide phase.

The crystal structure of Zn−LTM is related to the parent LDH. Both structures have, as a basic frame-

(32) Engelhard, G.; Michel, D. *High Resolution Solid State NMR of Silicates and Zeolites*; Wiley: New York, 1987.
(33) McKenzie, A. L.; Fishel, C. T.; Davis, R. J. *J. Catal.* **1992**, *138*, 547.

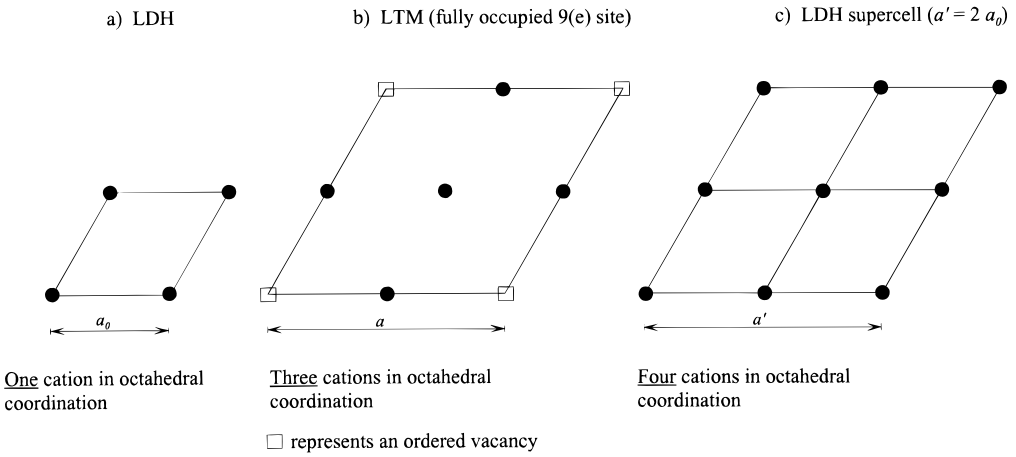

Figure 12. Variation in the number of cations in octahedral coordination resulting from *chimie douce* reaction.

work, sheets of zinc (and aluminum) octahedra running perpendicular to the *c* axis. The type and occupancy of the octahedral sites however, differ in the two structures. In the LDH framework, the metal cations fully occupy site 3(a), such that a_0 equals the cation−cation distance within the sheet (Figure 12a). However, in the Zn−LTM structure, the metal cations occupy site 9(e) with variable occupancy. Consequently, *a* for the LTM structure depends on the Mo−Mo distance, a distance equivalent to that between consecutive ordered vacancies at the origin (Figure 12b). In a LTM structure, there can be a maximum of three metal cations per layer in the unit cell. Typically, however, there are only two metal cations per layer in the unit cell, as is the case in Zn−LTM. If we define a supercell of the LDH with $a' = 2\ a_0$, $c' = c_0$, the area of the unit supercell would be almost identical with that of the LTM cell. In this equivalent area supercell however, there would be four metal cations per layer (Figure 12c). Therefore, the *chimie douce* synthesis reaction, while reconstructing the fundamental layered nature of the structure from the metastable zincite phase, reduces the number of octahedrally coordinated cations in the layers.

This reduction in the number of cations determined crystallographically complements the elemental analysis of the Zn−LTM phase. Elemental analysis had shown that the final product contained only 0.63% Al. This suggested that, on reaction with the ammonium heptamolybdate solution, the tetrahedral Al in the zincite phase left the solid phase and entered into solution. XPS analyses of the elemental composition of the surface region of calcined Mg−Al LDHs reported in the literature have indicated that the surface regions were enriched in Al.[33] This evidence, together with the ^{27}Al NMR data, suggests that the reactivity of the calcined Zn_4Al_2−LDH results from the presence of the tetrahedrally coordinated Al. On reaction, the Al enters into solution, thereby preventing the reconstruction of the LDH phase (which requires a positively charged framework resulting from trivalent cation substitution in the divalent lattice.) The loss of cations by this mechanism generates the vacancies in the octahedral sites of the oxide/hydroxide sheets required for the formation of the LTM structure.

Comparing the LTM structure with the LDH structure, it is interesting to note that the charge on the framework has been reversed. The LDH structure consists of positively charged sheets with intercalated anions such as CO_3^{2-} in the interlayer region. The LTM structure, however, consists of negatively charged layers, which leads to the incorporation of cations, e.g., NH_4^+, in the interlayer region. Therefore, this *chimie douce* reaction has changed not only the chemical and structural features of the LDH precursor but its electronic nature as well.

Conclusions

This paper describes a novel synthesis route for the preparation of a crystalline phase in which the structure and chemical composition of both the host and interlayer region of a layered precursor change. As a result of these changes, the product is a layered material that, in terms of charge, is a mirror image of its precursor. The room-temperature *chimie douce* synthesis technique produces layered transition-metal molybdate (LTM) materials from metastable mixed oxides derived from LDH precursors. The applicability of this synthesis route is dependent on the composition of the LDH, and it appears that metastability in the calcined LDH resulting from the presence of tetrahedrally coordinated aluminum favors conversion to the LTM phase.

The focus of this paper is the synthesis route by which Zn−LTM was prepared. This room-temperature *chimie douce* synthesis in which a crystalline phase was prepared from a metastable mixed oxide is exceptional in its chemistry. There is a remarkable confluence of chemical processes that have to occur in order to generate the LTM structure, including the rehydrolysis and dealumination of the mixed oxide, the formation of MoO_4^{2-} species from the heptamolybdate anion, and their migration into the interlayer region, the ordering of vacancies within the octahedral sheet, the capping of these vacancies by bonding of the tetrahedral molybdate species, and the incorporation of ammonium ions within the interlayer regions—all occurring at room temperature over a time frame of less than 2 h.

Acknowledgment. This work was supported by the National Science Foundation (CTS-9257223 and CTS-9411901). D.L. was partially funded by the Exxon Summer Intern Program. The authors would like to thank Dr. John Millar (Exxon) for the NMR analyses.

Supporting Information Available: Listings of crystal data (6 pages). Ordering information is given on any current masthead page.

CM950427I